



Flood disturbances  
using terrestrial  
photography

K. Džubáková et al.

This discussion paper is/has been under review for the journal Hydrology and Earth System Sciences (HESS). Please refer to the corresponding final paper in HESS if available.

# Monitoring of riparian vegetation response to flood disturbances using terrestrial photography

K. Džubáková<sup>1,2</sup>, P. Molnar<sup>1</sup>, K. Schindler<sup>3</sup>, and M. Trizna<sup>2</sup>

<sup>1</sup>Institute of Environmental Engineering, ETH Zurich, Zurich, Switzerland

<sup>2</sup>Department of Physical Geography and Geoecology, Comenius University in Bratislava, Bratislava, Slovakia

<sup>3</sup>Institute of Geodesy and Photogrammetry, ETH Zurich, Zurich, Switzerland

Received: 3 March 2014 – Accepted: 9 March 2014 – Published: 21 March 2014

Correspondence to: P. Molnar (molnar@ifu.baug.ethz.ch)

Published by Copernicus Publications on behalf of the European Geosciences Union.

Title Page

Abstract

Introduction

Conclusions

References

Tables

Figures



Back

Close

Full Screen / Esc

Printer-friendly Version

Interactive Discussion



## Abstract

The distribution of riparian vegetation on river floodplains is strongly impacted by floods. In this study we use a new setup with high resolution ground-based cameras in an Alpine gravel bed braided river to quantify the immediate response of riparian vegetation to flood disturbance with the use of vegetation indices. Five largest floods with return periods between 1.4 and 20.1 years in the period 2008–2011 in the Maggia River were used to evaluate patterns of vegetation response in three distinct floodplain units (main bar, secondary bar, transitional zone) and to compare seven vegetation indices. The results show both negative (damage) and positive (enhancement) response of vegetation in a short period following floods, with a selective impact based on the hydrogeomorphological setting and the intensity of the flood forcing. The spatial distribution of vegetation damage provides a coherent picture of floodplain response in the three floodplain units with different flood stress. We show that the tested vegetation indices generally agree on the direction of predicted change and its spatial distribution. The average disagreement between indices was in the range 14.4–24.9% despite the complex environment, i.e. highly variable surface wetness, high gravel reflectance, extensive water–soil–vegetation contact zones. We conclude that immediate vegetation response to flood disturbance may be effectively monitored by terrestrial photography with potential for long-term assessment in river management and restoration projects.

## 1 Introduction

Riverine environments are considered worldwide to be among the most threatened ecosystems due to flow regulation, water abstraction, and widespread channelization of rivers (Nilsson and Berggren, 2000; Tockner and Stanford, 2002). Riparian vegetation is under natural conditions a dynamic component of the riverine environment providing a range of important ecosystem services. Its composition and spatial distribution is largely determined by floodplain morphology and the hydrological regime of the river

**HESSD**

11, 3359–3385, 2014

## Flood disturbances using terrestrial photography

K. Džubáková et al.

[Title Page](#)

[Abstract](#)

[Introduction](#)

[Conclusions](#)

[References](#)

[Tables](#)

[Figures](#)

[⏪](#)

[⏩](#)

[◀](#)

[▶](#)

[Back](#)

[Close](#)

[Full Screen / Esc](#)

[Printer-friendly Version](#)

[Interactive Discussion](#)





**Flood disturbances  
using terrestrial  
photography**

K. Džubáková et al.

[Title Page](#)[Abstract](#)[Introduction](#)[Conclusions](#)[References](#)[Tables](#)[Figures](#)[⏪](#)[⏩](#)[◀](#)[▶](#)[Back](#)[Close](#)[Full Screen / Esc](#)[Printer-friendly Version](#)[Interactive Discussion](#)

2012). While various satellite data products are available on an almost daily basis, their rather coarse spatial resolution ( $\sim 10^1$  m) limits their use to reach-based analysis of larger river systems (Johansen et al., 2010; Bertoldi et al., 2011a; Parsons and Thoms, 2013). On the other hand, aerial photographs generally provide much better spatial resolution ( $\sim 10^0$  m) but a low sampling rate in time mainly due to high data acquisition costs (Verrelst et al., 2008; Bertoldi et al., 2011b; Caruso et al., 2013).

An alternative approach for detailed local analysis of riparian vegetation activity at the scale of individual gravel bars is terrestrial photography. This provides very high spatial resolution ( $< 10^0$  m) as well as a high sampling rate in time (daily or less). We are of the opinion that terrestrial photography is a viable approach for the continuous monitoring of riparian vegetation change as attested by emerging recent studies (e.g., Bertoldi et al., 2011b; Welber et al., 2012; Pasquale et al., 2014). In this paper we report the first results from ground-based photographic monitoring of riparian vegetation with high spatial detail on a gravel bar in the Maggia River in southern Switzerland.

Our system of two digital cameras serves as a broadband sensor for the monitoring of riparian vegetation in the visible and near infrared range. The imagery can be further processed into vegetation indices (VIs) defined as ratios of reflected radiation in the visible range related to photosynthetic and accessory pigments to reflected radiation in the near-infrared range associated with scattering processes by the leaf surface and internal structure (Bargain et al., 2013). Several VIs have been developed in the literature, each with their own advantages and disadvantages. The ratio vegetation index (RVI) and green RVI (GRVI) are conventional VIs, the normalized difference vegetation index (NDVI) and green NDVI (GNDVI) belong to differential indices. Both, RVI and NDVI are sensitive to optical properties of the soil background (Baret et al., 1991). Their sensitivity is even more pronounced with increasing sparseness of the vegetation cover (Eckert and Engesser, 2013) which is specific for riparian systems. To reduce the impact of soil reflectance, the soil-adjusted vegetation index (SAVI) and green SAVI (GSAVI) were developed (Huete, 1988), followed by the transformed SAVI (TSAVI) (Baret et al., 1991) and the modified SAVI (MSAVI) (Qi et al., 1994). Other

indices, such as the chlorophyll vegetation index (CVI) focus on the green band reflectance of plants (Ortiz et al., 2011). The vegetation indices we used in this study are listed in Table 1.

A survey of the literature shows that the choice of a vegetation index depends on the individual studied plants and purpose of analysis. Vegetation indices in agriculture are commonly used for mapping biophysical characteristics and plant vigor of single or few species. The question remains how to apply these methods to riparian vegetation monitoring in river floodplains with many species and intermittent plant cover on gravel bars, and are they robust enough to identify changes in vegetation cover and vigor immediately after floods. These two questions form the basis for this paper.

The main aims of this study are: (1) to analyze the spatial distribution and intensity of immediate vegetation response to large floods, where we aim to capture not only severe vegetation damage and erosion, but also the less apparent change of vegetation vigor; (2) to study the vegetation response in three distinct floodplain units of a gravel bar (main bar, secondary bar, transitional zone) which are meaningful units with regard to the concept of the floodplain mosaic system; and (3) to provide a comparison of vegetation indices for their use in the riverine environment. The analysis was performed for five floods in a four year period (2008–2011) on a gravel bar of an Alpine braided river (Maggia River, Switzerland). The relatively numerous flood events within the four study years enabled us to assess the vegetation response of the same species composition to different flood stages and longer term weather conditions.

## 2 Study area

Maggia is an Alpine river located in southeast Switzerland, north of the city of Locarno. The river originates at an altitude of about 2500 m, flows through Lake Naret (2310 m), Lake Sambuco (1461 m), and then south through the Maggia Valley into Lake Maggiore (193 m). The bedrock of the valley is formed by Penninic Crystalline Nappe predominantly covered by Holocene alluvial deposits. Within these settings Maggia evolved into

## Flood disturbances using terrestrial photography

K. Džubáková et al.

Title Page

Abstract

Introduction

Conclusions

References

Tables

Figures

⏪

⏩

◀

▶

Back

Close

Full Screen / Esc

Printer-friendly Version

Interactive Discussion



a braided river system with a gravel cobble bed occasionally covered with fine sediment deposits on elevated alluvial bars. The average bed slope is about 0.8 %.

The hydrological regime of the river is significantly influenced by hydropower infrastructure (dams, intakes, canals) constructed in the upper watershed in the 1950s. Since then, approximately 75 % of the natural river flow has been diverted to the power station Verbano at Lake Maggiore and only minimum flows are released into the main valley. At present, the bypassed section has an average daily streamflow of  $4.1 \text{ m}^3 \text{ s}^{-1}$ , while it was close to  $16 \text{ m}^3 \text{ s}^{-1}$  prior to 1954 (Molnar et al., 2008). The 100 year flood peak is estimated at  $768 \text{ m}^3 \text{ s}^{-1}$  (Bignasco) at the upper end of our study reach. The hydropower system regulation practically removes the snowmelt spring-summer flow peak in the valley, but does not affect the largest floods appreciably, mainly due to the upstream location of reservoirs and their relatively low storage capacity. As a consequence, floods with a perceptible impact on riparian vegetation still occur on the average more than once per year in the main valley (Perona et al., 2009a).

In this study we focused on the 500 m long and 300–400 m wide reach of the river in the main valley located between the villages Someo and Giumaglio. Three distinct floodplain units were identified within the study reach, namely main gravel bar (MB), secondary gravel bar (SB), and a transitional zone (TZ) (Fig. 1). The main bar is the largest, most elevated unit. It is located in the center of the floodplain in close proximity to the main channel. The secondary bar is at the edge of the floodplain. Both bars are separated by a transitional zone with very active channel dynamics. The secondary channel in the transitional zone is fully connected with the main channel only during the largest flood events.

The vegetation composition within the study reach is heterogeneous. The dominant *Salix* species are *Salix purpurea*, *Salix alba*, *Salix eleagnos*, often accompanied by *Populus nigra* and *Alnus incana*, occasionally by *Acer pseudoplatanus*, *Tilia cordata*, *Fallopia sachalinensis*, and *Robinia pseudoacacia*. The tree height varies from 1 to 10 m. Sparsely distributed herbaceous cover is located in the inner part of the bars with sand accumulation. The variability in the vegetation composition within the three

## Flood disturbances using terrestrial photography

K. Džubáková et al.

Title Page

Abstract

Introduction

Conclusions

References

Tables

Figures

◀

▶

◀

▶

Back

Close

Full Screen / Esc

Printer-friendly Version

Interactive Discussion



studied floodplain units is notable. *Salix* individuals are located at the upstream part of MB, and towards its inner part are often accompanied by *Populus*. Unlike on MB, *Salix* is predominantly mixed with *Fallopia* on SB. Although fewer in number, the largest diversity in species is found in TZ with *Alnus*, *Salix*, locally *Populus* and *Acer*.

## 3 Data and methods

### 3.1 Meteorological and hydrological data

Hourly records of solar radiation, air temperature, relative humidity, and rainfall used in this study were obtained from the weather station Locarno-Monti (MeteoSwiss), located about 15 km downstream from the study reach. Hourly streamflow is gauged on the Maggia River at Bignasco (FOEN) approximately 7.8 km upstream of the study reach. There is an ungauged small tributary (Rovana) between the gauging station and our study reach, thus the peak flows of the studied floods in our reach are a lower estimate.

We analysed the five largest summer floods in the period 2008–2011 with return periods between 1.4 and 20.1 years (Table 2). The upstream part of the MB and the TZ were submerged during all studied floods, the SB and central part of the MB were submerged only in 2011.

The meteorological conditions and streamflow before and after each flood are summarized in Fig. 2. The flood in May 2008 was the earliest in the season with the lowest air temperature (minimum 10 °C) and the highest relative humidity prior to the event. The raingauge at Locarno-Monti did not capture the storm rainfall which occurred mostly in the headwaters of the catchment. With the flood peak of 192 m<sup>3</sup> s<sup>-1</sup>, it was the smallest but at the same time the longest flood analysed. There were two floods with similar peaks in 2009. The summer of 2009 was very dry and hot, air temperatures prior to both floods reached or exceeded 30 °C, relative humidity was generally very low. The flood in June had intense rainfall (40 mm h<sup>-1</sup>) measured in Locarno-Monti and the flood peak reached 254 m<sup>3</sup> s<sup>-1</sup>. The subsequent flood in July was preceded by three days of

## Flood disturbances using terrestrial photography

K. Džubáková et al.

Title Page

Abstract

Introduction

Conclusions

References

Tables

Figures

◀

▶

◀

▶

Back

Close

Full Screen / Esc

Printer-friendly Version

Interactive Discussion



moderately intense rainfall ( $20 \text{ mm h}^{-1}$ ) and reached a flood peak of  $272 \text{ m}^3 \text{ s}^{-1}$ . The flood in June 2010 occurred during a period with average air temperature around  $20^\circ \text{C}$  and high relative humidity. With the flow reaching  $301 \text{ m}^3 \text{ s}^{-1}$  it was the second largest analysed flood. The raingauge in Locarno-Monti captured the storm event only partially, while heaviest precipitation occurred in the upper basin. The largest flood in June 2011 also occurred during a period with average air temperature slightly above  $20^\circ \text{C}$ . Intense rainfall covered the entire basin and was measured at Locarno-Monti with intensities about  $40 \text{ mm h}^{-1}$  for a short duration. The flood peak reached  $598 \text{ m}^3 \text{ s}^{-1}$ .

### 3.2 Image collection and processing

The camera installation in the Maggia River consists of two digital cameras (Canon EOS 350D, 24 mm lens and 8 Mpx CCD sensor) positioned 530 m above the floodplain. The horizontal distance to the study reach is between 860 and 1460 m. The first camera is a regular camera recording the R, G, B visual bands. The second camera is adjusted to be sensitive in the near-infrared range. The UV/IR blocking filter on the sensor has been replaced with a clear filter and a 850 nm IR filter (heliopan IR850) was placed on the lens. The red band gives us the NIR band for vegetation index analysis. Photographs are taken automatically every day at 11:00 UTC in CRW format from summer 2008. All camera settings (focus, aperture, etc.) were set manually to the best average lightning conditions in the valley. More details of the installation can be found in Molnar et al. (2014).

Image processing was performed in Matlab. The images were converted to TIFF 48-bit format and registered using a cross-correlation algorithm. Images with significant light limitations due to haze or high relative humidity were automatically identified based on their color histograms and excluded from further analysis. Seven VIs (Table 1) were computed and the VI images were subsequently orthorectified. The image resolution after orthorectification was 0.5 m, thus individual shrubs and trees on the gravel bar are easily visible.

## Flood disturbances using terrestrial photography

K. Džubáková et al.

Title Page

Abstract

Introduction

Conclusions

References

Tables

Figures

⏪

⏩

◀

▶

Back

Close

Full Screen / Esc

Printer-friendly Version

Interactive Discussion



Two orthorectification methods were tested. While planar orthorectification defined by five rectification points of distinct fluvial features resulted in an evenly distributed image distortion of 1–2 pixels ( $< 1$  m), the orthorectification based on a LiDAR DEM (2 m resolution) was better in areas with reliable LiDAR points but significantly distorted ( $\sim 2.5$  m) in zones with decreased LiDAR DEM accuracy. Since our study reach is indeed a very flat surface, we decided to apply planar orthorectification in our analysis. The image distortion is acceptable for studying individual riparian trees and patches which have footprints much greater than 1 m.

### 3.3 Vegetation index analysis

The flood impact on riparian vegetation was evaluated by comparison of VIs from a period before and after each flood event. To obtain a statistically robust measure of the vegetation activity we defined the before-flood  $VI^{bf}(t)$  and post-flood  $VI^{pf}(t)$  arrays as

$$VI^{bf}(t) = \text{median}(VI(t - k); k = 1, \dots, 7), \quad (1)$$

$$VI^{pf}(t) = \text{median}(VI(t + k); k = 1, \dots, 7), \quad (2)$$

where  $VI(t)$  is the vegetation index value on day  $t$  and the median is computed pixel-wise. We chose the median VI pixel value for a period  $k$  before and after each flood in order to reduce the potential impact of adverse light conditions and shadows on the images in individual days. We experimented with different  $k$  values and found that  $k = 7$  days provided an acceptable smoothing without destroying the signal in the data.

We then computed the difference between the two arrays to get the vegetation change array

$$\Delta VI(t) = VI^{pf}(t) - VI^{bf}(t). \quad (3)$$

Negative values of  $\Delta VI$  indicate a decrease in the vegetation index after the flood, e.g. by the erosion and damage of vegetation, while positive values indicate an increase in the vegetation index after the flood, e.g. rise in photosynthetic activity and growth.

Title Page

Abstract

Introduction

Conclusions

References

Tables

Figures

◀

▶

◀

▶

Back

Close

Full Screen / Esc

Printer-friendly Version

Interactive Discussion



To compare the indices we took the vegetation change array for each flood for a pair of indices  $\Delta VI_1$  and  $\Delta VI_2$ , and we estimated an index of disagreement as

$$ID(t)_{1,2} = \text{area}(\Delta VI_1(t) \cdot \Delta VI_2(t) < 0) / \text{total area.} \quad (4)$$

5 The index of disagreement ID between all floods was averaged and is reported in Table 3 for all VI index pairs. For further analysis we used the index that gives on the average the lowest disagreement with all the other indices in terms of the direction of predicted vegetation change, i.e. overall vegetation damage ( $\Delta VI < 0$ ) and enhancement ( $\Delta VI > 0$ ). The assumption is that all analyzed vegetation indices reliably represent  
10 vegetation activity and that the differences among the indices will occur mainly on the water–soil–vegetation contact zones due to their different sensitivity.

## 4 Results

### 4.1 Comparison of vegetation indices

15 To quantify the vegetation response to floods we first report the overall comparison of the VIs by the index of disagreement in Table 3. The results show that the chosen VIs capture the trends of vegetation response (i.e. vegetation damage or enhancement) coherently, as the pair-wise differences of the indices vary between 0.7 and 32.2%. Generally, the indices based on the same visible band tend to show more similar results in comparison to indices based on different visible bands. The RVI and GRVI differ by  
20 only 0.7% from their normalized derivatives NDVI and GNDVI, and by 10.1–12.3% from the soil-adjusted derivatives SAVI and GSAVI. On average, GNDVI (14.4%) and GRVI (14.5%) have the lowest disagreement with the other indices, while CVI (24.9%) differs the most.

## Flood disturbances using terrestrial photography

K. Džubáková et al.

Title Page

Abstract

Introduction

Conclusions

References

Tables

Figures

⏪

⏩

◀

▶

Back

Close

Full Screen / Esc

Printer-friendly Version

Interactive Discussion



## 4.2 Vegetation response in time

Vegetation response measured by  $\Delta VI$  conditioned on the pre-flood vegetation vigor and river morphology gives us the most complete picture of the nature of flood-induced vegetation change. In Fig. 3 we show the boxplots of  $\Delta VI$  as a function of the pre-flood  $VI^{bf}$  for the three floodplain units and five floods using the GNDVI. Only pixels with vegetation cover, i.e.  $VI^{bf} > 0.15$  are considered in the analysis.

The first result comes from the statistical distribution of  $VI^{bf}$  for the floodplain units which shows that most vegetation is growing on the main bar, considerably less on the secondary bar and in the transitional zone. All three floodplain units exhibit modes at  $VI^{bf} = 0.3\text{--}0.4$ , which correspond to healthy and large individual plants. Vegetation with  $VI^{bf} = 0.4\text{--}0.5$ , i.e. the highest computed VI, is present in all three floodplain units, especially in the transitional zone. Comparing the pre-flood vegetation conditions for the period 2008–2011, the vegetation composition appears to be reasonably stable, there is limited evidence for widespread scouring or vegetation growth in all three floodplain units at this temporal scale. Scouring of a small extent is visible between the flood in 2008 and 2009.

The second result is the detailed effect of the individual floods. Riparian vegetation tends to be both damaged and enhanced after each flood at the floodplain unit scale. Vegetation with lower  $VI^{bf}$  responds to flood disturbance with greater absolute change for the smaller floods. At the same time, while vegetation damage occurs for all  $VI^{bf}$  categories, vegetation enhancement is more likely to occur for vegetation with higher  $VI^{bf}$ , i.e. stronger and larger plants. This indicates a selective destructive effect on smaller or weaker plants and enhancement for stronger individuals.

Perhaps most striking is the difference between the intensity of vegetation response to the first four smaller floods and to the largest flood in July 2011. The first four floods show on average rather small changes, while the flood in 2011 shows considerably greater impact on vegetation, changes as high as  $\Delta VI = -0.4$  indicating complete removal of plants. These erosive effects have however not affected the strongest plants,

HESSD

11, 3359–3385, 2014

### Flood disturbances using terrestrial photography

K. Džubáková et al.

Title Page

Abstract

Introduction

Conclusions

References

Tables

Figures

⏪

⏩

◀

▶

Back

Close

Full Screen / Esc

Printer-friendly Version

Interactive Discussion



in fact the areas with highest pre-flood  $VI^{bf}$  have experienced an enhancement of the VI index in the week following the flood, especially on the main bar.

### 4.3 Spatial distribution of vegetation response

The intensity of the vegetation response to floods differs between the floodplain units. The main bar has moderate response with  $\Delta VI$  mostly between  $-0.1$  and  $0.1$  (outliers excluded) for the first four floods and between  $-0.2$  and  $0.15$  for the flood in 2011. The secondary bar has slightly smaller vegetation response than the main bar. The exception is the response after the flood in 2011, where significant damage is evident for low  $VI^{bf}$ . Unlike the vegetation response on the bars, the  $\Delta VI$  range in the transitional zone fluctuates considerably more, from  $-0.2$  to  $0.15$  for the first four floods, and from  $-0.4$  to  $0.2$  for the flood in 2011.

The spatial distribution of  $\Delta VI$  is shown in Fig. 4. The area with the most negatively affected vegetation appears to be the transitional zone and the contact zone between the main bar and the river. On the other hand, vegetation enhancement is characteristic for the central parts of the main bar.

The flood in May 2008 with its long duration early in the vegetation season caused a similar intensity but a slightly different spatial distribution of vegetation response compared to the following floods. The different vegetation response might have also been impacted by the presence of plants in close proximity to the main channel and on the top of the transitional zone that were scoured in autumn 2008. Particularly interesting is the impact of the shortest analysed flood in July 2009 that occurred only one month after the flood in June 2009. It was the only flood with widespread vegetation enhancement, most likely associated with surface water supply to a floodplain dried by the hot summer. The largest flood in 2011 is the only analysed flood which caused severe vegetation damage, local scour, mostly on the upper part of the main alluvial bar and in the transitional zone. Despite the predominantly destructive impact of this

## Flood disturbances using terrestrial photography

K. Džubáková et al.

Title Page

Abstract

Introduction

Conclusions

References

Tables

Figures

⏪

⏩

◀

▶

Back

Close

Full Screen / Esc

Printer-friendly Version

Interactive Discussion



flood, the inner most elevated parts of the main bar also show significant vegetation enhancement, probably caused by wetting of the inundated surfaces.

## 5 Discussion

The vegetation indices in this study were estimated for a heterogeneous and highly dynamic riverine environment characterized by a mixture of gravel and water surfaces, and riparian vegetation with different density and reflectance properties. This is a very challenging environment compared to traditional single-species applications in agriculture (e.g. Mulla, 2012; Vincini et al., 2008). Despite the specifics of the riverine environment, i.e. variable surface wetness, high gravel reflectance, and extensive water–soil–vegetation contact zones, the estimation of vegetation response by the different indices varied reasonably (14.4–24.9% on average). Figure 4 shows the level of agreement between the seven studied indices in detecting vegetation damage  $\Delta VI < 0$  in space for the individual floods. The results show that there is substantial coherence in the spatial predictions of changes by the VIs, even for the largest flood in 2011, which is a promising result for applications in riparian environments.

Differences between indices using the same visible band, e.g. NDVI and SAVI, have been explained in the literature (e.g. Jackson and Huete, 1991). Particular to our interest is the fact that in our study the indices using the red visible band tended to have noticeably more similar results than indices based on the green visible band. As the red visible band is more sensitive to chlorophyll in healthy leaves, while the green visible band is more sensitive to chlorophyll in weakened leaves (Gitelson et al., 1996), we presume that the indices based on different visible bands are differently sensitive to various plants and their response to floods. We conclude that although all studied VIs did appear to capture essential information on vegetation change coherently, future work should be directed at understanding the nature of the differences between them connected to details of vegetation water stress on floodplains (e.g. Parsons and Thoms, 2013).

## Flood disturbances using terrestrial photography

K. Džubáková et al.

Title Page

Abstract

Introduction

Conclusions

References

Tables

Figures

◀

▶

◀

▶

Back

Close

Full Screen / Esc

Printer-friendly Version

Interactive Discussion



## Flood disturbances using terrestrial photography

K. Džubáková et al.

Title Page

Abstract

Introduction

Conclusions

References

Tables

Figures

⏪

⏩

◀

▶

Back

Close

Full Screen / Esc

Printer-friendly Version

Interactive Discussion



Considering the general trend of vegetation response, prevailing damage of vegetation with low  $VI^{bf}$  and enhancement of vegetation with high  $VI^{bf}$  indicate connections between vegetation stability, growth, and vigour. Smaller plants on surfaces exposed to more frequent and damaging stress during flood inundation have a harder time to recover between floods (Perona et al., 2012), while more protected locations on the gravel bar and floodplain provide a better environment for plants to germinate and grow. This supports the spatial distribution of riparian vegetation on floodplain surfaces (Gurnell et al., 2012). Additional complexity is added to this picture by the sediment structure. The presence of fine material in the substrate and a coarse gravel layer on the surface inhibiting evaporation have been shown to be critical for maintaining a high soil moisture after inundation (Meier and Hauer, 2010) and will likely impact the degree of vegetation enhancement following floods.

The floodplain units displayed different vegetation composition and response to floods. The main bar was the most vegetated area with the most variable spatial pattern of vegetation response to flood disturbances. The vegetation on the secondary bar had generally lower index values than the vegetation on the main bar despite the fact that it is flooded less often than the vegetation on the main bar. The transitional zone was found to be the zone with the most vigorous and diverse, but at the same time the most sensitive vegetation within the floodplain. The results are in accord with the understanding of the floodplain as a mosaic system, where each floodplain unit is determined by its specific morphological, hydrological, and biotic site conditions (Bendix and Hupp, 2000; Jacobson, 2013). Our study suggests that the mosaic-like organization of vegetation is perhaps not only valid in a long-term perspective as shown in previous literature, but also on short flood time scales.

## 6 Conclusions

This study demonstrated the use of a high resolution ground-based camera monitoring of riparian vegetation in an Alpine gravel bed braided river. The focus was on

quantifying the immediate response of riparian vegetation to flood disturbance by standard vegetation indices.

The results offer new insights into the complexity of riparian vegetation dynamics within a floodplain. The main results from a study of 5 largest floods with return periods between 1.4 and 20.1 years in the period 2008–2011 on a reach in the gravel bed braided Maggia River in Switzerland were: (1) Riparian vegetation displays both negative (damage) and positive (enhancement) response in a short period after floods. There is evidence for a selective impact based on the hydrogeomorphological setting and the flood forcing, with destructive effects on smaller or weaker plants and enhancement for stronger individuals higher up on the floodplain. (2) The intensity and spatial distribution of vegetation damage provides a coherent picture of the floodplain response in three distinct units (main bar, secondary bar, transitional zone) with different inundation potential and flood stress. A threshold effect is apparent, with the largest flood in 2011 producing by far the greatest change. (3) We demonstrated that standard vegetation indices provide a means to quantify vegetation response even in this heterogeneous environment characterized by a mixture of gravel and water surfaces and riparian vegetation with different density and reflectance properties. The seven tested indices agreed on the direction of change and its spatial distribution despite many site specifics, e.g. variable surface wetness, high gravel reflectance, and extensive water–soil–vegetation contact zones, with a disagreement on the average only between 14.4 and 24.9%.

One of the main aims of this paper was to provide a first analysis of a ground-based camera monitoring setup which provides high spatial and temporal resolution of riparian vegetation change at a gravel-bar and river reach scale. The resolution provides a considerable advantage over remote sensing by satellites with the downside connected to the broadband nature of the reflectance data. A practical advantage of such a system are low purchasing and maintenance costs. We are convinced that such systems are suitable for long-term monitoring of riparian areas and have high potential for river management, particularly for regulated rivers or rivers with restoration projects.

**Flood disturbances  
using terrestrial  
photography**

K. Džubáková et al.

Title Page

Abstract

Introduction

Conclusions

References

Tables

Figures



Back

Close

Full Screen / Esc

Printer-friendly Version

Interactive Discussion



*Acknowledgements.* This research was funded by the Scientific Exchange Program Sciex-NMS Grant 12.111, the Slovak Research and Development Agency Grant APVV-0625-11, and the Slovak Scientific Grant Agency VEGA Project 1/0937/11. Meteorological data was provided by MeteoSwiss (Federal Office of Meteorology and Climatology). Hydrological data were provided by FOEN (Federal Office for the Environment). We particularly thank Ondrej Budac (EPFL, Switzerland) for his technical support.

## References

- Amoros, C. and Bornette, G.: Connectivity and biocomplexity in waterbodies of riverine floodplains, *Freshwater Biol.*, 47, 761–776, 2002. 3361
- Auble, G. T., Friedman, J. M., and Scott, M. L.: Relating riparian vegetation to present and future streamflows, *Ecol. Appl.*, 4, 544–554, 1994. 3361
- Ballesteros, J. A., Bodoque, J. M., Diez-Herrero, A., Sanchez-Silva, M., and Stoffel, M.: Calibration of floodplain roughness and estimation of flood discharge based on tree-ring evidence and hydraulic modelling, *J. Hydrol.*, 403, 103–115, 2011. 3361
- Baret, F., Guyot, G., and Major, D. J.: TSAVI: a vegetation index which minimizes soil brightness effects on LAI and APAR estimation, in: Proceedings of the 12th Canadian symposium on remote sensing and IGARSS, Vancouver, Canada, 10–14 July 1989, 1355–1358, 1991. 3362
- Bargain, A., Robin, M., Méléder, V., Rosa, P., Le Menn, E., Harin, N., and Barillé, L.: Seasonal spectral variation of *Zostera noltii* and its influence on pigment-based Vegetation Indices, *J. Exp. Mar. Biol. Ecol.*, 446, 86–94, 2013. 3362
- Bendix, J.: Stream power influence on Southern Californian riparian vegetation, *J. Veg. Sci.*, 10, 243–252, 1999. 3361
- Bendix, J. and Hupp, C. R.: Hydrological and geomorphological impacts on riparian plant communities, *Hydrol. Process.*, 14, 2977–2990, 2000. 3361, 3372
- Bertoldi, W., Drake, N. A., and Gurnell, A. M.: Interactions between river flows and colonizing vegetation on a braided river: exploring spatial and temporal dynamics in riparian vegetation cover using satellite data, *Earth Surf. Proc. Land.*, 36, 1474–1486, 2011a. 3361, 3362
- Bertoldi, W., Gurnell, A. M., and Drake, N. A.: The topographic signature of vegetation development along a braided river: results of a combined analysis of airborne lidar,



## Flood disturbances using terrestrial photography

K. Džubáková et al.

Title Page

Abstract

Introduction

Conclusions

References

Tables

Figures

◀

▶

◀

▶

Back

Close

Full Screen / Esc

Printer-friendly Version

Interactive Discussion

- Gurnell, A. M. and Petts, G.: Hydrology and ecology of river systems, in: *Treatise on Water Science*, edited by: P. Wilderer, Elsevier, Oxford, 237–269, ISBN 9780444531995, 2011. 3361
- Gurnell, A. M., Bertoldi, W., and Corenblit, D.: Changing river channels: the roles of hydrological processes, plants and pioneer fluvial landforms in humid temperate, mixed load, gravel bed rivers, *Earth-Sci. Rev.*, 11, 129–141, 2012. 3361, 3372
- Huete, A. R.: A soil adjusted vegetation index (SAVI), *Remote Sens. Environ.*, 25, 295–309, 1988. 3362, 3379
- Jackson, R. D. and Huete, A. R.: Interpreting vegetation indices, *Prev. Vet. Med.*, 11, 185–200, 1991. 3371
- Jacobson, R. B.: Riverine habitat dynamics, in: *Treatise on Geomorphology*, edited by: Shroder, J. F., Academic Press, San Diego, 6–19, ISBN 9780080885223, 2013. 3372
- Johansen, K., Phinn, S., and Witte, C.: Mapping of riparian zone attributes using discrete return LiDAR, QuickBird and SPOT-5 imagery: assessing accuracy and costs, *Remote Sens. Environ.*, 114, 2679–2691, 2010. 3362
- Latterell, J. J., Scott Bechtold, J., O’Keefe, T. C., Pelt, R., and Naiman, R. J.: Dynamic patch mosaics and channel movement in an unconfined river valley of the Olympic Mountains, *Freshwater Biol.*, 51, 523–544, 2006. 3361
- Loheide, S. P. and Booth, E. G.: Effects of changing channel morphology on vegetation, groundwater, and soil moisture regimes in groundwater-dependent ecosystems, *Geomorphology*, 126, 364–376, 2011. 3361
- Meier, C. I. and Hauer, F. R.: Strong effect of coarse surface layer on moisture within gravel bars: results from an outdoor experiment, *Water Resour. Res.*, 46, W05507, doi:10.1029/2008WR007250, 2010. 3372
- Merritt, D. M., Scott, M. L., Poff, L. N., and Auble, G. T., and Lytle, D. A.: Theory, methods and tools for determining environmental flows for riparian vegetation: riparian vegetation-flow response guilds, *Freshwater Biol.*, 55, 206–225, 2010. 3361
- Molnar, P., Favre, V., Perona, P., Burlando, P., Randin, C., and Ruf, W.: Floodplain forest dynamics in a hydrologically altered mountain river, *Peckiana*, 5, 17–24, 2008. 3364
- Molnar, P., Burlando, P., Corripio, J., Perona, P., and Dzubakova, K.: Continuous monitoring of riparian vegetation in the Maggia with digital photography, *Geophys. Res. Lett.*, in review, 2014. 3366

## Flood disturbances using terrestrial photography

K. Džubáková et al.

Title Page

Abstract

Introduction

Conclusions

References

Tables

Figures

◀

▶

◀

▶

Back

Close

Full Screen / Esc

Printer-friendly Version

Interactive Discussion



- Mulla, D. J.: Twenty five years of remote sensing in precision agriculture: key advances and remaining knowledge gaps, *Biosyst. Eng.*, 114, 358–371, 2012. 3361, 3371
- Nilsson, C. and Berggren, K.: Alterations of riparian ecosystems caused by river regulation, *BioScience*, 50, 783–792, 2000. 3360
- 5 Ortiz, B. V., Thomson, S. J., Huang, Y., Reddy, K. N., and Ding, W.: Determination of differences in crop injury from aerial application of glyphosate using vegetation indices, *Comput. Electron. Agr.*, 77, 204–213, 2011. 3363
- Parsons, M. and Thoms, M. C.: Patterns of vegetation greenness during flood, rain and dry resource states in a large, unconfined floodplain landscape, *J. Arid Environ.*, 88, 24–38, 10 2013. 3362, 3371
- Pasquale, N., Perona, P., Francis, R., and Burlando, P.: Effects of streamflow variability on the vertical root density distribution of willow cutting experiments, *Ecological Eng.*, 40, 167–172, 2012. 3361
- Pasquale, N., Perona, P., Wombacher, A., and Burlando, P.: Hydrodynamic model calibration 15 from pattern recognition of non-orthorectified terrestrial photographs, *Comput. Geosci.*, 62, 160–167, 2014. 3362
- Perona, P., Molnar, P., Savina, M., and Burlando, P.: An observation-based stochastic model for sediment and vegetation dynamics in the floodplain of an Alpine braided river, *Water Resour. Res.*, 45, W09418, doi:10.1029/2008WR007550, 2009a. 3361, 3364
- 20 Perona, P., Camporeale, C., Perucca, E., Savina, M., Molnar, P., Burlando, P., and Ridolfi, L.: Modelling river and riparian vegetation interactions and related importance for sustainable ecosystem management, *Aquat. Sci.*, 71, 266–278, 2009b. 3361
- Perona, P., Molnar, P., Crouzy, B., Perucca, E., Jiang, Z., McLelland, S., and Gurnell, A. M.: Biomass selection by floods and related timescales: Part 1. Experimental observations, 25 *Adv. Water Resour.*, 39, 85–96, 2012. 3361, 3372
- Pringle, C. M., Naiman, R. J., and Bretschko, G.: Patch dynamics in lotic systems: the stream as a mosaic, *J. N. Am. Benthol. Soc.*, 7, 503–524, 1988. 3361
- Qi, J., Chebouni, A., Huete, A. R., Kerr, Y. H., and Sorooshian, S.: A modified soil adjusted vegetation index, *Remote Sens. Environ.*, 48, 119–126, 1994. 3362
- 30 Rouse Jr., J. W., Haas, R. H., Deering, D. W., Schell, J. A., and Harlan, J. C.: Monitoring the vernal advancement and retrogradation (green wave effect) of natural vegetation, NASA/GSFC Type III Final Report, Texas A&M Univ., College Station, Greenbelt, MD, 1974. 3379

## Flood disturbances using terrestrial photography

K. Džubáková et al.

Title Page

Abstract

Introduction

Conclusions

References

Tables

Figures

⏪

⏩

◀

▶

Back

Close

Full Screen / Esc

Printer-friendly Version

Interactive Discussion



- Sripada, R. P., Schmidt, J. P., Dellinger, A. E., and Beegle, D. B.: Evaluating multiple indices from a canopy reflectance sensor to estimate corn N requirements, *Agron. J.*, 100, 1553–1561, 2008. 3379
- 5 Stoffel, M., Butler, D. R., and Corona, C.: Mass movements and tree rings: a guide to dendrogeomorphic field sampling and dating, *Geomorphology*, 200, 106–120, 2013. 3361
- Tal, M. and Paola, C.: Effects of vegetation on channel morphodynamics: results and insights from laboratory experiments, *Earth Surf. Proc. Land.*, 35, 1014–1028, 2010. 3361
- Tockner, K. and Stanford, J. A.: Riverine flood plains: present state and future trends, *Environ. Conserv.*, 29, 308–330, doi:10.1017/S037689290200022X, 2002. 3360
- 10 Toda, Y., Ikeda, S., Kumagai, K., and Asano, T.: Effects of flood flow on flood plain soil and riparian vegetation in a gravel river, *J. Hydraul. Eng.-ASCE*, 131, 950–960, 2005. 3361
- Verrelst, J., Schaepman, M. E., Koetz, B., and Kneubühler, M.: Angular sensitivity analysis of vegetation indices derived from CHRIS/PROBA data, *Remote Sens. Environ.*, 112, 2341–2353, 2008. 3362
- 15 Vincini, M., Frazzi, E., and D'Alessio, P.: A broad-band leaf chlorophyll vegetation index at the canopy scale, *Precis. Agric.*, 9, 303–319, 2008. 3371, 3379
- Welber, M., Bertoldi, W., and Tubino, M.: The response of braided planform configuration to flow variations, bed reworking and vegetation: the case of the Tagliamento River, Italy, *Earth Surf. Proc. Land.*, 37, 572–582, 2012. 3362

## Flood disturbances using terrestrial photography

K. Džubáková et al.

**Table 1.** Overview of the vegetation indices (VIs) used in this study. NIR, R, and G stand for the spectral reflectance in the near-infrared, visible red and visible green frequencies.  $L$  is a scaling constant, assigned the value 0.5.

	Vegetation Index	Formula	Reference
RVI	Red VI	$\text{NIR}/\text{R}$	Birth and Mcvey (1968)
GRVI	Green Ratio VI	$\text{NIR}/\text{G}$	Sripada et al. (2008)
NDVI	Normalized Difference VI	$(\text{NIR} - \text{R})/(\text{NIR} + \text{R})$	Rouse et al. (1974)
GNDVI	Green Normalized Difference VI	$(\text{NIR} - \text{G})/(\text{NIR} + \text{G})$	Gitelson et al. (1996)
SAVI	Soil Adjusted VI	$(1 + L)(\text{NIR} - \text{R})/(\text{NIR} + \text{R} + L)$	Huete (1988)
GSAVI	Green Soil Adjusted VI	$(1 + L)(\text{NIR} - \text{G})/(\text{NIR} + \text{G} + L)$	Sripada et al. (2008)
CVI	Chlorophyll VI	$\text{NIR} \cdot \text{R}/\text{G}^2$	Vincini et al. (2008)

[Title Page](#)
[Abstract](#)
[Introduction](#)
[Conclusions](#)
[References](#)
[Tables](#)
[Figures](#)
[Back](#)
[Close](#)
[Full Screen / Esc](#)
[Printer-friendly Version](#)
[Interactive Discussion](#)


## Flood disturbances using terrestrial photography

K. Džubáková et al.

**Table 2.** Analysed floods in this study in the period 2008–2011. The return period of flood peaks is estimated from data for the period 1982–2011 at Bignasco (Source: Meteoswiss and FOEN).

Flood Date	No. of images before/after	Peak $\text{m}^3 \text{s}^{-1}$	Return period yrs
28 May 2008	2/4	192	1.4
6 Jun 2009	7/6	254	1.7
17 Jul 2009	6/7	272	1.9
12 Jun 2010	4/2	301	2.2
13 Jul 2011	5/6	598	20.1

[Title Page](#)
[Abstract](#)
[Introduction](#)
[Conclusions](#)
[References](#)
[Tables](#)
[Figures](#)
[Back](#)
[Close](#)
[Full Screen / Esc](#)
[Printer-friendly Version](#)
[Interactive Discussion](#)


## Flood disturbances using terrestrial photography

K. Džubáková et al.

**Table 3.** Index of Disagreement (ID) in % of the total number of pixels where two VIs disagree on the direction of vegetation change, i.e. vegetation damage or enhancement.

	NDVI	GNDVI	RVI	GRVI	SAVI	GSAVI	CVI	Mean
NDVI		17.9	0.7	17.9	10.1	22.1	31.9	16.8
GNDVI	17.9		17.9	0.7	20.4	12.3	17.3	14.4
RVI	0.7	17.9		17.8	10.3	22.2	31.9	16.8
GRVI	17.9	0.7	17.8		20.5	12.5	17.4	14.5
SAVI	10.1	20.4	10.3	20.5		18.3	32.2	18.6
GSAVI	22.1	12.3	22.2	12.5	18.3		18.9	17.7
CVI	31.9	17.3	31.9	17.4	32.2	18.9		24.9

Title Page

Abstract

Introduction

Conclusions

References

Tables

Figures

◀

▶

◀

▶

Back

Close

Full Screen / Esc

Printer-friendly Version

Interactive Discussion



Flood disturbances  
using terrestrial  
photography

K. Džubáková et al.

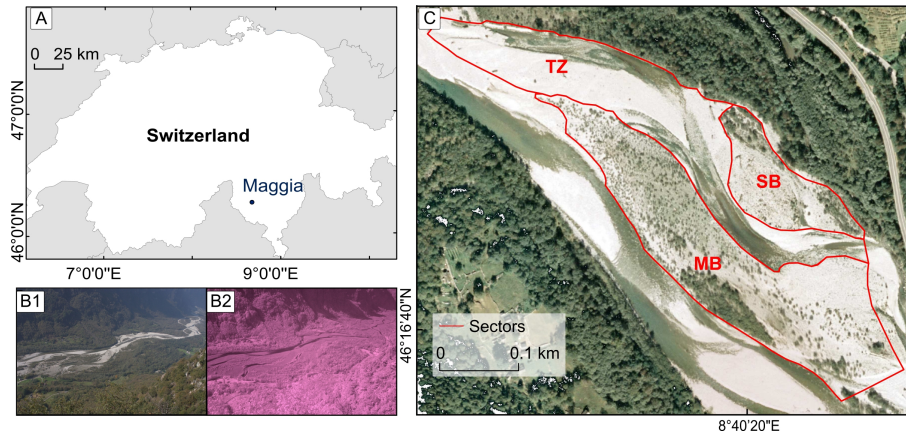


**Fig. 1.** (A) Study reach location within Switzerland, (B) Maggia valley view from the cameras (B1: VIS, B2: IR ), (C) study reach subdivided into three sectors: main alluvial bar (MB), secondary alluvial bar (SB), transitional zone (TZ).

[Title Page](#)[Abstract](#)[Introduction](#)[Conclusions](#)[References](#)[Tables](#)[Figures](#)[⏪](#)[⏩](#)[◀](#)[▶](#)[Back](#)[Close](#)[Full Screen / Esc](#)[Printer-friendly Version](#)[Interactive Discussion](#)

## Flood disturbances using terrestrial photography

K. Džubáková et al.

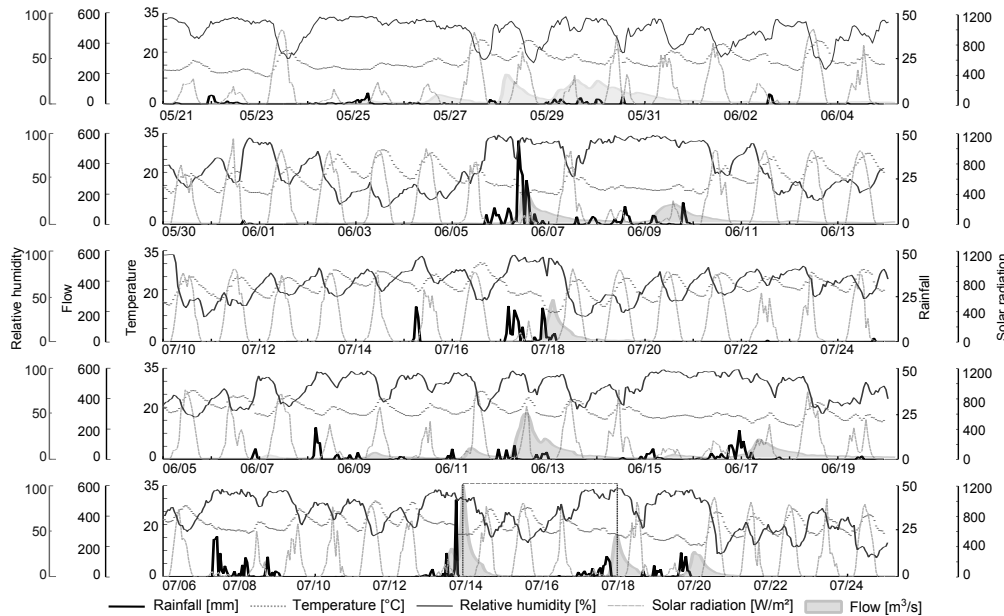


**Fig. 2.** Meteorological and hydrological conditions seven days before and after each flood. Floods are arranged according to Table 2, from top (2008) to bottom (2011).

[Title Page](#)

[Abstract](#)

[Introduction](#)

[Conclusions](#)

[References](#)

[Tables](#)

[Figures](#)

⏪

⏩

⏴

⏵

[Back](#)

[Close](#)

[Full Screen / Esc](#)

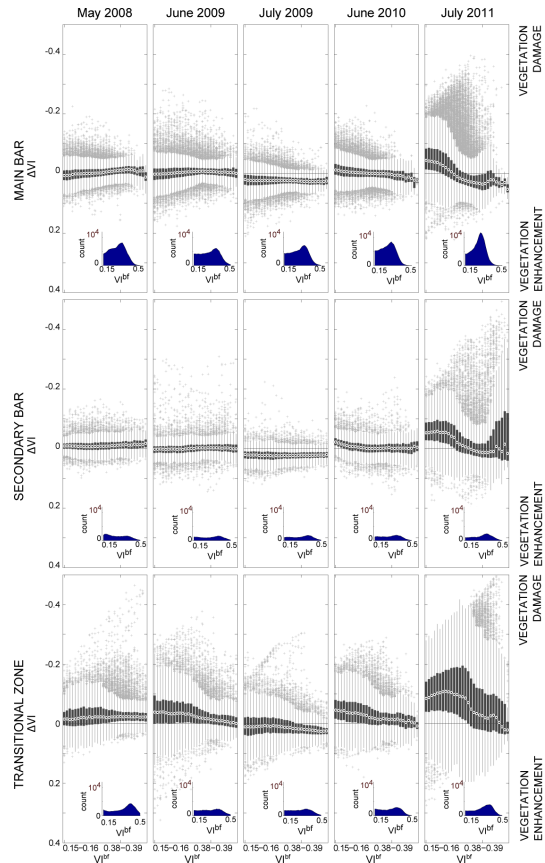
[Printer-friendly Version](#)

[Interactive Discussion](#)



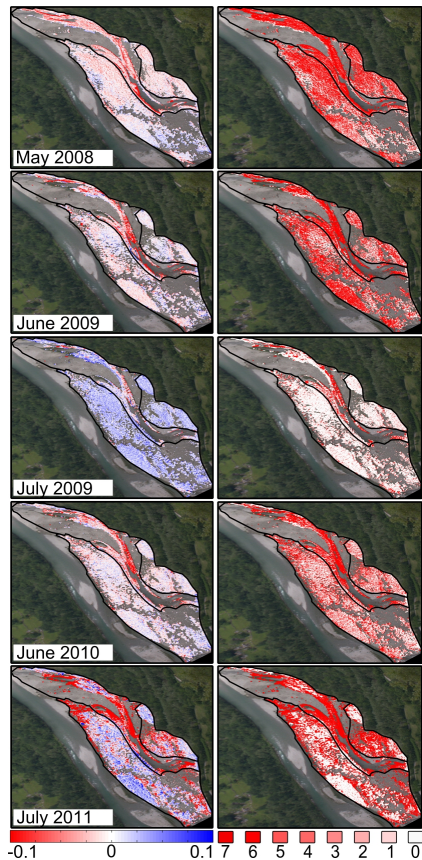
## Flood disturbances using terrestrial photography

K. Džubáková et al.



**Fig. 3.** Box plots for vegetation response  $\Delta VI$  with respect to the VI recorded before flood.  $\Delta VI < 0$  indicates vegetation damage and  $\Delta VI > 0$  vegetation enhancement. Points are drawn as outliers if they are larger than  $q_3 + 1.5(q_3 - q_1)$  or smaller than  $q_1 - 1.5(q_3 - q_1)$ , where  $q_1$  and  $q_3$  are the 25th and 75th percentiles, respectively.

[Title Page](#)
[Abstract](#)
[Introduction](#)
[Conclusions](#)
[References](#)
[Tables](#)
[Figures](#)
[◀](#)
[▶](#)
[◀](#)
[▶](#)
[Back](#)
[Close](#)
[Full Screen / Esc](#)
[Printer-friendly Version](#)
[Interactive Discussion](#)

**Fig. 4.** Left column: spatial distribution of vegetation response  $\Delta VI$  to each flood.  $\Delta VI < 0$  indicates vegetation damage and  $\Delta VI > 0$  vegetation enhancement. Right column: number of VIs indicating vegetation damage for each flood. Base image: swisstopo image from 1 June 2008.

## Flood disturbances using terrestrial photography

K. Džubáková et al.

Title Page

Abstract

Introduction

Conclusions

References

Tables

Figures

◀

▶

◀

▶

Back

Close

Full Screen / Esc

Printer-friendly Version

Interactive Discussion

